

# TRPC3 induces intervertebral disc degeneration by mediating the Ca<sup>2+</sup>/NF-κB pathway to inhibit autophagy

Yingchao Gao<sup>1,A,D–F</sup>, Ning Zhang<sup>2,B,C,F</sup>, Jun-Fei Zhang<sup>3,B,C,F</sup>, Zhengqi Fei<sup>1,A,E,F</sup>

<sup>1</sup> Department of Orthopedics, 942<sup>nd</sup> Hospital of the Joint Logistics Support Force of the People's Liberation Army of China, Yinchuan, China

<sup>2</sup> Department of Orthopedics, General Hospital of Ningxia Medical University, Yinchuan, China

<sup>3</sup> School of Clinical Medicine, Ningxia Medical University, Yinchuan, China

A – research concept and design; B – collection and/or assembly of data; C – data analysis and interpretation;

D – writing the article; E – critical revision of the article; F – final approval of the article

Advances in Clinical and Experimental Medicine, ISSN 1899–5276 (print), ISSN 2451–2680 (online)

Adv Clin Exp Med. 2026;35(5):819–833

## Address for correspondence

Yingchao Gao

E-mail: jirui.999@163.com

## Funding sources

This study was supported by the Ningxia Natural Science Foundation (grant No. 2021AAC03413) and the Joint Logistic Support Force 942 Hospital Research Program (grant No. D942YKY0003).

## Conflict of interest

None declared

Received on January 20, 2025

Reviewed on May 18, 2025

Accepted on June 25, 2025

Published online on May 5, 2026

## Cite as

Gao Y, Zhang N, Zhang JF, Fei Z. TRPC3 induces intervertebral disc degeneration by mediating the Ca<sup>2+</sup>/NF-κB pathway to inhibit autophagy. *Adv Clin Exp Med*. 2026;35(5):819–833. doi:10.17219/acem/207572

## DOI

10.17219/acem/207572

## Copyright

Copyright by Author(s)

This is an article distributed under the terms of the Creative Commons Attribution 3.0 Unported (CC BY 3.0) (<https://creativecommons.org/licenses/by/3.0/>)

## Abstract

**Background.** Intervertebral disc degeneration (IDD) is the primary cause of lower back pain. Transient receptor potential canonical 3 (*TRPC3*) is a nonselective cation channel permeable to Ca<sup>2+</sup>.

**Objectives.** This study explores the mechanisms by which the *TRPC3*-mediated Ca<sup>2+</sup>/nuclear factor kappa B (NF-κB) pathway regulates autophagy in IDD.

**Materials and methods.** An IDD rat model was established using the annulus fibrosus puncture method and was treated with local intraspinal injection of adeno-associated virus (AAV)-shRNA targeting *TRPC3*. Primary human nucleus pulposus cells (NPCs) were transfected with *TRPC3* siRNA and subsequently treated with pyrrolidine dithiocarbamate (PDTC; an NF-κB inhibitor), rapamycin (RAPA), or 3-methyladenine (3-MA), respectively. Micro-computed tomography (micro-CT), hematoxylin and eosin (H&E) staining, immunohistochemistry, western blotting, transmission electron microscopy (TEM), and flow cytometry were performed.

**Results.** *TRPC3* expression was significantly increased in IDD rats ( $p < 0.05$ ). *TRPC3* shRNA ameliorated histopathological damage in IDD rats and promoted the expression of autophagy-related protein 5 (*ATG5*), *Beclin-1*, and *LC3-II* (all  $p < 0.05$ ). In vitro, interleukin-1 beta (*IL-1β*) increased Ca<sup>2+</sup> levels, siRNA *TRPC3* reduced them, and PDTC further decreased them ( $p < 0.05$ ). In addition, siRNA *TRPC3* increased the expression of *ATG5*, *Beclin-1*, and the *LC3-II/LC3-I* ratio and inhibited phosphorylation of *p*-NF-κB *p65* in NPCs ( $p < 0.05$ ). Transmission electron microscopy and flow cytometry showed that siRNA *TRPC3*-induced autophagy promoted apoptosis in NPCs ( $p < 0.05$ ). Furthermore, siRNA *TRPC3* increased the levels of aggrecan and collagen II and decreased matrix metalloproteinase-13 (*MMP-13*) expression ( $p < 0.05$ ).

**Conclusions.** *TRPC3* exacerbates IDD by inhibiting protective autophagy via activation of the Ca<sup>2+</sup>/NF-κB signaling pathway. Knockdown of *TRPC3* promotes autophagy, which in turn influences NPC apoptosis and extracellular matrix (ECM) metabolism. This study offers potential novel strategies for IDD prevention and treatment.

**Key words:** autophagy, NF-κB, intervertebral disc degeneration, *TRPC3*, calcium ions influx

## Highlights

- *TRPC3* is upregulated in intervertebral disc degeneration (IDD), driving pathological  $\text{Ca}^{2+}$  influx and activation of the NF- $\kappa$ B signaling pathway in nucleus pulposus cells.
- Silencing *TRPC3* restores autophagy in IDD, significantly increasing *ATG5*, *Beclin-1*, and *LC3-II* expression while reducing NF- $\kappa$ B p65 phosphorylation.
- *TRPC3* inhibition improves disc matrix homeostasis, enhancing aggrecan and collagen II levels and suppressing *MMP-13*-mediated extracellular matrix (ECM) degradation.
- Targeting the *TRPC3*/ $\text{Ca}^{2+}$ /NF- $\kappa$ B axis represents a novel therapeutic strategy for preventing and treating IDD.

## Background

Low back pain (LBP) is the most common chronic musculoskeletal condition affecting adults and has emerged as a leading cause of global disability, profoundly impacting patients' work capacity and daily life.<sup>1</sup> Research indicates that 60–80% of individuals experience symptoms of LBP, with approx. 10% of patients becoming disabled.<sup>2–4</sup> Currently, approx. 630 million people worldwide suffer from neck pain and LBP. Intervertebral disc degeneration (IDD) is the primary cause of LBP and disc-related disorders, such as herniation and spinal stenosis.<sup>5</sup> Studies have revealed that approx. 40% of low back and leg pain cases are attributable to IDD.<sup>6</sup> The prevalence of IDD is steadily increasing across all age groups, posing significant challenges for medical care and society.<sup>7</sup> Although IDD is particularly prevalent among the elderly population, a shift toward younger patients has been observed in recent years, likely due to changes in lifestyle and habits.<sup>8</sup> Intervertebral disc degeneration is a progressive, multifactorial condition characterized by biomechanical, structural, and biological changes in disc tissue induced by various factors, ultimately leading to the loss of disc integrity and function. These changes include annulus fibrosus rupture, nucleus pulposus (NP) herniation, extracellular matrix (ECM) degradation, reduced disc height, and compression of the spinal cord and nerve roots, ultimately resulting in lower back and leg pain.<sup>9</sup> Recent research suggests that IDD is a complex disease resulting from the interaction of multiple factors, including aging, genetic predisposition, mechanical stress, inflammation, oxidative stress, metabolic dysfunction, environmental factors, and autophagy.<sup>5,10–12</sup> Furthermore, IDD is characterized by degeneration of the intervertebral disc ECM, leading to reduced biomechanical integrity and pain.<sup>13</sup> Among these factors, matrix metalloproteinases (MMPs) are key contributors to ECM degradation in IDD. Previous studies have shown that bovine bone grafts can contribute to intervertebral disc repair by supporting cell attachment, proliferation, and matrix synthesis.<sup>14</sup> Recent studies have also demonstrated that inhibition of matrix degradation can reduce mitochondrial damage, inhibit cell apoptosis and senescence, and significantly delay the progression of IDD.<sup>15</sup> However, the pathogenesis of IDD remains a major challenge

in clinical practice. Therefore, it is crucial to further elucidate the mechanisms underlying IDD and identify reliable therapeutic targets to improve ECM metabolic imbalance and ultimately reverse the progression of IDD.

As an intracellular recycling process, autophagy degrades cytoplasmic components via lysosomes and plays a vital role in cellular self-degradation and recycling.<sup>16</sup> This process is essential for maintaining metabolic homeostasis. It has been reported that autophagy alleviates osteoarthritis by regulating ECM metabolism.<sup>17</sup> Recent studies have increasingly demonstrated that autophagy plays a crucial role in IDD.<sup>18,19</sup> Cheng et al. has found that regulation of chaperone-mediated autophagy can effectively delay the progression of IDD in an inflammatory environment.<sup>20</sup> However, the role of autophagy in IDD remains controversial because of its dual effects. Some studies have reported that the expression levels of autophagy-associated genes are significantly higher in IDD than in healthy discs.<sup>21</sup> In addition, research has indicated that appropriate activation of autophagy can protect nucleus pulposus cells (NPCs), which are the core cellular components of the intervertebral disc, from pressure-induced damage. In contrast, impairment of autophagic function can lead to apoptosis of NPCs, thereby further accelerating the progression of IDD.<sup>22,23</sup>

Transient receptor potential (TRP) channels are known for their involvement in sensory processes, such as temperature and pain perception, as well as in the regulation of cellular calcium homeostasis. Transient receptor potential canonical 3 (*TRPC3*) is a  $\text{Ca}^{2+}$ -permeable, nonselective cation channel that plays vital roles in a wide range of cellular physiological processes. *TRPC3* facilitates calcium entry, thereby enabling cells to regulate gene expression, as well as cell growth and differentiation. Notably, *TRPC3* has been implicated in various physiological and pathological conditions, including cardiovascular diseases, neurological disorders, and cancer. In the context of IDD, the specific mechanisms of *TRPC3* remain controversial. Some studies suggest that *TRPC3* is involved in cytosolic  $\text{Ca}^{2+}$  elevation, activation of nuclear factor kappa B (NF- $\kappa$ B), and cytokine upregulation.<sup>24</sup> Notably, research has shown that increased *TRPC3* expression can lead to elevated intracellular  $\text{Ca}^{2+}$  concentrations and is associated with decreased bone mass.<sup>25</sup> Abnormal *TRPC3* channel activity may promote bone resorption, reduce bone

density, and mediate the  $\text{Ca}^{2+}$ /NF- $\kappa$ B signaling pathway.<sup>26</sup> Calcium ( $\text{Ca}^{2+}$ ) is one of the most abundant and important signaling molecules in the human body. In tissues such as intervertebral discs, bone, and cartilage, elevated intracellular  $\text{Ca}^{2+}$  concentrations activate  $\text{Ca}^{2+}$  signaling pathways, which in turn regulate gene expression and protein synthesis, thereby influencing changes in the microenvironment of intervertebral disc tissue. Previous investigations have demonstrated the critical role of  $\text{Ca}^{2+}$  signaling in intervertebral disc tissues. Intervertebral disc degeneration leads to alterations in the osmotic pressure of intervertebral disc tissue, resulting in activation of the  $\text{Ca}^{2+}$  signaling pathway. Intervertebral disc cells regulate gene expression and protein synthesis by increasing intracellular  $\text{Ca}^{2+}$  concentrations. Furthermore,  $\text{Ca}^{2+}$  acts as a second messenger in the human body, activating downstream signaling pathways. The role of the NF- $\kappa$ B signaling pathway in IDD has been widely recognized; however, its upstream regulatory mechanisms are diverse. Evidence suggests that calcium/calmodulin-dependent protein kinase II, in conjunction with interleukin-1 receptor-associated kinase 1 (*IRAK1*), plays a critical role in the phosphorylation processes that activate NF- $\kappa$ B.<sup>27</sup> When activated, the NF- $\kappa$ B pathway triggers cell apoptosis and ECM degradation, thereby promoting IDD.<sup>28</sup> In addition, the NF- $\kappa$ B pathway promotes autophagy in various diseases. Melatonin has been shown to induce autophagy via the NF- $\kappa$ B signaling pathway, thereby preventing ECM degradation in intervertebral disc cells.<sup>29</sup> Furthermore, through the *miR-139-3p/CXCR4/NF- $\kappa$ B* axis, *lncRNA H19* enhances autophagy and apoptosis in NPCs, thereby aggravating IDD.<sup>30</sup> However, there are currently no reports on whether *TRPC3* can activate autophagy to regulate IDD via the  $\text{Ca}^{2+}$ /NF- $\kappa$ B pathway. Moreover, whether *TRPC3*-induced NF- $\kappa$ B activation through  $\text{Ca}^{2+}$  influx exerts synergistic effects on apoptosis and ECM degradation remains to be further elucidated.

## Objectives

This study aims to investigate the role and underlying mechanisms by which the *TRPC3*-mediated  $\text{Ca}^{2+}$ /NF- $\kappa$ B pathway inhibits autophagy in IDD using both in vivo and in vitro approaches.

## Materials and methods

### Animals

Twenty-four specific pathogen-free (SPF) healthy male Sprague Dawley (SD) rats (8 weeks old; body weight,  $200 \pm 20$  g) were purchased from Chengdu Dashuo Biotechnology Co., Ltd. (Chengdu, China). The rats were housed in a pathogen-free environment for 1 week to acclimate to the laboratory conditions, with free access to a standard

diet (caloric composition: 70% carbohydrate, 10% fat, and 24% protein; provided by Chengdu Dashuo Biotechnology Co., Ltd.) and water, under a normal 12-h light/dark cycle.

## Experimental design

The rats were randomly assigned to 4 groups: the sham group ( $n = 6$ ), model group ( $n = 6$ ), shRNA negative control (NC) group ( $n = 6$ ), and shRNA *TRPC3* group ( $n = 6$ ). An IDD rat model was established using the annulus fibrosus puncture method.<sup>31</sup> Twelve hours before model induction, the rats were fasted with ad libitum access to water. The rats were weighed and then intraperitoneally injected with 40 mg/kg of 1% pentobarbital sodium for anesthesia, based on body weight. Once anesthetized, the rats were placed in the supine position with their limbs immobilized. The surgical area was shaved and disinfected with iodine. A longitudinal incision of 3–4 cm was made approx. 0.5 cm to the right of the midline. Each tissue layer was sequentially incised to expose the posterior abdominal wall. The intestinal tract and greater omentum were gently retracted to prevent injury, and the paravertebral lumbar muscles were bluntly dissected. The L4/5 and L5/6 intervertebral discs were exposed, and a 21-gauge needle was used to puncture the annulus fibrosus at 3 points on the right anterior aspect of the vertebral body, directed toward the center of the intervertebral disc. The puncture depth was approx. 2–3 mm, limiting the injury to the full thickness of the annulus fibrosus. Following the injury, the needle was maintained in position for 10 s. After successful puncture, the incision was closed in layers. Rats in the sham surgery group underwent the same skin and tissue incision without intervertebral disc puncture. Postoperatively, routine care was provided, including intramuscular injection of penicillin ( $8 \times 10^5$  U/day, once daily for 3 consecutive days) to prevent infection. The rats were closely monitored postoperatively for food intake, gait, wound infection, and urinary retention.

Three rats were randomly selected from the sham and model groups at 8 weeks after surgery. The rats were anesthetized with isoflurane, followed by cervical dislocation at the atlantoaxial joint. Tissue samples were collected, and the skin, paravertebral muscles, and ligaments were dissected layer by layer. The L5/6 intervertebral disc tissue was rapidly harvested and fixed in 4% paraformaldehyde. To evaluate the success of model establishment and observe morphological changes, hematoxylin and eosin (H&E) staining was performed.

Model establishment was confirmed by pathological examination at 8 weeks after surgery. On the 1<sup>st</sup> day after successful model establishment, rats in the shRNA NC group received a local intraspinal injection of adeno-associated virus (AAV)-shRNA NC ( $1 \times 10^{12}$   $\mu\text{g}/\text{kg}$ ). Rats in the shRNA *TRPC3* group received a local intraspinal injection of AAV-shRNA *TRPC3* ( $1 \times 10^{12}$   $\mu\text{g}/\text{kg}$ ). Both AAV-shRNA NC and AAV-shRNA *TRPC3* were designed and synthesized by Shanghai Jikai Gene Medical Technology Co., Ltd.

(Shanghai, China). After 3 weeks, the rats were anesthetized with an overdose of isoflurane, and NP tissue samples were collected from the intervertebral discs of each group.

## H&E staining

Intervertebral disc tissues were first decalcified using a 15% ethylenediaminetetraacetic acid (EDTA) solution. The tissues were then dehydrated and embedded, sectioned at a thickness of 5  $\mu\text{m}$ , stained with hematoxylin for 10–20 min followed by eosin for 3–5 min, and mounted with neutral gum.<sup>32</sup> Images were acquired using a Panoramic 250 FLASH III digital slide scanner (3DHISTECH, Budapest, Hungary).

## Immunohistochemistry staining

Intervertebral disc tissues were sectioned, deparaffinized, and rehydrated. The sections were then heated in 10 mM sodium citrate buffer (pH 6.0) at 100°C for 30 min for antigen retrieval and blocked with 3% bovine serum albumin (BSA; cat. No. GC305010; Servicebio, Wuhan, China) for 1 h at room temperature. The sections were subsequently incubated overnight at 4°C with primary antibodies against autophagy-related protein 5 (*ATG5*; bs-4005R, 1:100; Proteintech, Wuhan, China), *Beclin-1* (11306-1-AP, 1:100, Proteintech), and *LC3-II* (14600-1-AP, 1:200; Proteintech). Afterward, the sections were incubated with a secondary antibody (horseradish peroxidase (HRP)-labeled goat anti-rabbit immunoglobulin G (IgG; H+L) GB23303, 1:100; Servicebio) for 1 h at room temperature. Diaminobenzidine (DAB) color development and hematoxylin counterstaining were then performed.<sup>33</sup> Finally, the sections were examined under a light microscope (BA400Digital; Motic China Group Co., Ltd., Xiamen, China), and images were captured using a digital trinocular microscope (BA400 Digital; McAudi, Xiamen, China).

## Micro-computed tomography scan

Intervertebral disc tissue samples were scanned using the Micro-CT Scanner software. For three-dimensional analysis, the samples were analyzed using CTAn software (Bruker Micro-CT, Billerica, USA) to obtain the following parameters: structure model index (SMI), trabecular thickness (Tb.Th), bone volume to total volume ratio (BV/TV), trabecular number (Tb.N), and trabecular separation (Tb.Sp).

## Primary human NPCs isolation and culture

Nucleus pulposus tissue was obtained during lumbar discectomy, and its morphology was observed under a light microscope (Leica DM11; Leica Microsystems, Wetzlar, Germany). Following washing with phosphate-buffered

saline (PBS), NP tissue samples were digested with 0.25% trypsin and 0.2% collagenase type II at 37°C for 4–6 h. After removal of tissue debris by filtration through a 200- $\mu\text{m}$  filter, purified NPCs were cultured in Dulbecco's modified Eagle's medium (DMEM)/F-12 supplemented with 10% fetal bovine serum (FBS), 100  $\mu\text{g}/\text{mL}$  streptomycin, and 100  $\mu\text{g}/\text{mL}$  penicillin at 37°C in a humidified atmosphere containing 5%  $\text{CO}_2$ . Nucleus pulposus cells at passage 2 were used for subsequent in vitro experiments.

## Cell transfection and grouping

The cell experiments were divided into 2 parts.

Part I: NPCs were divided into the following groups: control, IL-1 $\beta$ , IL-1 $\beta$  + siRNA NC, IL-1 $\beta$  + siRNA *TRPC3*, and IL-1 $\beta$  + siRNA *TRPC3* + pyrrolidine dithiocarbamate (PDTc; NF- $\kappa$ B inhibitor, 100  $\mu\text{mol}/\text{L}$ ).

Part II: NPCs were divided into the following groups: control, IL-1 $\beta$ , IL-1 $\beta$  + siRNA NC, IL-1 $\beta$  + siRNA *TRPC3*, IL-1 $\beta$  + siRNA *TRPC3* + 3-methyladenine (3-MA; autophagy inhibitor), and IL-1 $\beta$  + siRNA *TRPC3* + rapamycin (RAPA; autophagy activator).

Cell transfection was performed using the RiboFect™ CP Transfection Kit (C10511-05; RiboBio, Guangzhou, China). The lyophilized siRNA was reconstituted in RNase-free water to obtain a 20  $\mu\text{M}$  stock solution. The transfection mixture was prepared by thoroughly mixing 120  $\mu\text{L}$  of RiboFect™ CP Buffer, 12  $\mu\text{L}$  of RiboFect™ CP Reagent, and 10  $\mu\text{L}$  of siRNA, followed by incubation at 37°C. Except for the control group, cells in all other groups were treated with 10 ng/mL IL-1 $\beta$  after cell adherence to induce cellular injury. Simultaneously, cells in the IL-1 $\beta$  + siRNA *TRPC3* + 3-MA group were treated with 3-MA (5 mmol/L), and cells in the IL-1 $\beta$  + siRNA *TRPC3* + RAPA group were treated with RAPA (250 nmol/L). The corresponding assays were performed 24 h later.

## Western blot

Rat intervertebral disc NP tissue or NPCs were lysed for 10 min in radioimmunoprecipitation assay (RIPA) lysis buffer (Beyotime, Shanghai, China). Protein concentrations were quantified using a bicinchoninic acid (BCA) Protein Assay Kit (Beyotime). Protein samples from the supernatant were mixed with an equal volume of sodium dodecyl sulfate (SDS) loading buffer and boiled for 5 min to denature the proteins. Equal amounts of protein were loaded onto a 12% polyacrylamide gel and subjected to electrophoresis for 60–90 min. Subsequently, proteins were transferred onto polyvinylidene fluoride (PVDF) membranes (Merck Millipore, Billerica, USA). To block nonspecific binding, the membranes were incubated with 5% skim milk for 1 h at room temperature. The PVDF membranes were then incubated with primary antibodies overnight at 4°C, followed by incubation with secondary antibodies for 2 h at room temperature.

The antibodies used were as follows: anti- $\beta$ -actin (cat. No. AC026, 1:50,000), anti-*ATG5* (cat. No. A0203, 1:1,000), anti-*Beclin-1* (cat. No. A7353, 1:2,000), anti-*LC3B* (cat. No. A19665, 1:2,000), anti-*NF- $\kappa$ B p65* (cat. No. A2547, 1:2,000), anti-phospho-*NF- $\kappa$ B p65* (cat. No. AP0123, 1:2,000), and anti-*MMP13* (cat. No. A11148, 1:2,000), all purchased from ABclonal Biotechnology Co., Ltd. (Wuhan, China); anti-*TRPC3* (cat. No. 77934, 1:1,000) was purchased from Cell Signaling Technology (CST; Danvers, USA); anti-aggregran (cat. No. DF7561, 1:1,000) and goat anti-rabbit IgG (H+L) HRP (cat. No. S0001, 1:5,000) were purchased from Affinity Biosciences (Beijing, China); and anti-collagen II (cat. No. BS-10589R, 1:2,000) was purchased from Bioss Biotechnology Co., Ltd. (Beijing, China).

Protein bands were visualized using an enhanced chemiluminescence (ECL) kit (Biosharp, Hefei, China), and signals were captured using the Tanon 5200 Multi-System (Tanon, Shanghai, China).

### Transmission electron microscope for autophagy observation

A transmission electron microscope (TEM) was used to investigate autophagy in NPCs. First, the NPC samples were subjected to primary fixation with 3% glutaraldehyde to preserve cellular structures. Subsequently, secondary fixation was performed using 1% osmium tetroxide to enhance contrast of the cellular components. Ultrathin sections with a thickness of approximately 60 nm were prepared using an ultramicrotome (Leica Camera AG). To improve electron density and visualization of cellular organelles, the sections were stained with uranyl acetate for 15 min. Subsequently, the sections were briefly stained with lead citrate for 2 min to further enhance contrast. Finally, the stained samples were examined using a JEM-1400 FLASH transmission electron microscope (JEOL, Tokyo, Japan).

### Detection of cell apoptosis by flow cytometry

To assess the apoptotic status of NPCs, flow cytometric analysis was performed using the Annexin V-APC/PI Apoptosis Detection Kit (KGA1030; KeyGen Biotech Corp., Ltd., Nanjing, China) according to the manufacturer's instructions.<sup>34</sup> Nucleus pulposus cells were seeded in 6-well plates at a density of  $2 \times 10^5$  cells per well and incubated at 37°C in a humidified atmosphere containing 5% CO<sub>2</sub> to allow cell attachment and growth. Once the cells reached appropriate confluency, apoptosis detection was initiated. A total of 5  $\mu$ L of Annexin V-FITC and 5  $\mu$ L of propidium iodide (PI) were added to the cell suspension. The cells were then incubated for 15 min at room temperature in the dark to allow effective binding of the dyes to the cell membranes. After incubation, the stained NPCs were analyzed using a flow cytometer (CytoFLEX; Beckman Coulter, Brea, USA).

## Statistical analyses

For statistical analysis, IBM SPSS Statistics v. 25 (IBM Corp., Armonk, USA) was used, and data are presented as the median (minimum–maximum). The Kruskal–Wallis (K–W) test, followed by Dunn's post hoc test with Bonferroni correction, was applied for multiple-group comparisons. A  $p < 0.05$  was considered statistically significant. Statistical analysis results are presented in Supplementary Tables 1–6.

## Results

### Inhibition of *TRPC3* improved histopathological damage in IDD rats

To investigate the role and mechanisms of *TRPC3* in IDD, AAV-shRNA *TRPC3* was injected into the intervertebral disc tissue of rats in the animal study. First, intervertebral disc tissues were evaluated using micro-CT, as shown in Table 1. Compared with the sham group, the model group exhibited decreased BV/TV, Tb.N, and Tb.Th values, while Tb.Sp and SMI were increased; however, only BV/TV, Tb.N, and SMI showed statistically significant differences (all  $p = 0.050$ ). However, no significant difference was observed between the shRNA *TRPC3* group and the shRNA NC group ( $p = 0.127$ ,  $p = 0.513$ ,  $p = 0.275$ ). To further evaluate histopathological changes, H&E staining was performed. In the model group, a significant reduction in NPCs was observed compared with the sham group, whereas chondrocytes and the cartilaginous matrix were increased and arranged in clusters. The shRNA NC group did not exhibit notable improvement in pathological conditions compared with the model group. In contrast, the shRNA *TRPC3* group exhibited a relatively intact intervertebral disc tissue structure: the annulus fibrosus was arranged in concentric circles with multiple layers of fibrocartilage and showed a denser organization, and the NP was rich in elastic gel-like material, with abundant NPCs and ECM, indicating attenuation of pathological

Table 1. Microstructural parameters of intervertebral disc tissue analyzed with micro-CT

Group	Sham	Model	shRNA NC	shRNA <i>TRPC3</i>
BV/TV [%]	37.44 $\pm$ 1.67	30.74 $\pm$ 1.95 <sup>#</sup>	30.17 $\pm$ 2.59	32.49 $\pm$ 1.25
Tb.N [mm]	3.51 $\pm$ 0.07	2.93 $\pm$ 0.24 <sup>#</sup>	2.92 $\pm$ 0.22	3.07 $\pm$ 0.04
Tb.Th [mm]	0.11 $\pm$ 0.002	0.10 $\pm$ 0.003	0.10 $\pm$ 0.005	0.11 $\pm$ 0.013
Tb.Sp [mm]	0.25 $\pm$ 0.01	0.28 $\pm$ 0.05	0.28 $\pm$ 0.02	0.26 $\pm$ 0.01
SMI	0.21 $\pm$ 0.09	0.82 $\pm$ 0.14 <sup>#</sup>	0.79 $\pm$ 0.17	0.64 $\pm$ 0.12

CT – computed tomography; BV/TV – percent bone volume; Tb.Th – trabecular thickness; Tb.Sp – trabecular separation; Tb.N – trabecular number; SMI – structure model index. Data were analyzed using the Kruskal–Wallis test followed by Dunn's post hoc test with Bonferroni correction; <sup>#</sup> $p < 0.05$ , compared with the sham group.

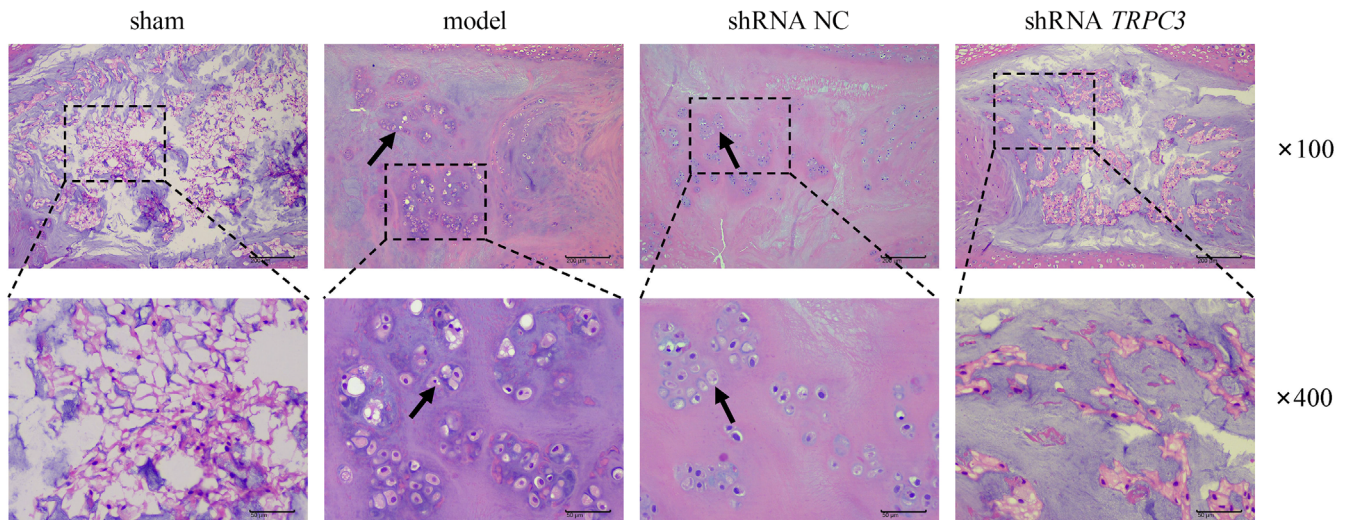


**Fig. 1.** Inhibition of *TRPC3* ameliorates histopathological damage in intervertebral disc degeneration (IDD) rats. Hematoxylin and eosin (H&E) staining was used to observe pathological changes in intervertebral disc tissues. Scale bars = 50  $\mu\text{m}$  ( $\times 400$ ) and 200  $\mu\text{m}$  ( $\times 100$ ). Black arrows indicate reduced numbers of NPCs and increased chondrocytes and cartilaginous matrix

*TRPC3* – transient receptor potential canonical 3; NC – negative control; NPCs – nucleus pulposus cells.

damage (Fig. 1). Therefore, these results indicate that *TRPC3* knockdown can ameliorate histopathological damage in IDD rats in vivo.

### Inhibition of *TRPC3* promoted autophagy in the nucleus pulposus of intervertebral discs in vivo

Subsequently, we analyzed the effect of shRNA *TRPC3* on autophagy levels in the NP of intervertebral discs in IDD rats using IHC staining. The expression levels of *ATG5*, *Beclin-1*, and *LC3-II* were markedly higher in the model group than in the sham group (all  $p = 0.050$ ). Moreover, treatment with AAV-shRNA *TRPC3* further increased the expression of *ATG5*, *Beclin-1*, and *LC3-II* compared with the shRNA NC group (all  $p = 0.050$ ) (Fig. 2, Supplementary Table 1). In addition, the model group exhibited a marked increase in *TRPC3* expression in NP tissue compared with the sham group, as confirmed by western blot analysis ( $p = 0.05$ ). In contrast, *TRPC3* expression levels were significantly decreased in the AAV-shRNA *TRPC3*-treated group relative to the shRNA NC group ( $p = 0.024$ ) (Fig. 3, Supplementary Table 2). Overall, these findings suggest that high *TRPC3* expression may lead to abnormal accumulation of autophagosomes by inhibiting autophagy, thereby aggravating IDD, whereas *TRPC3* knockdown may reverse the IDD phenotype by activating protective autophagy signaling.

### The knockdown of *TRPC3* inhibited the $\text{Ca}^{2+}$ /NF- $\kappa\text{B}$ pathway to promote autophagy in NPCs in vitro

To further investigate the mechanisms by which *TRPC3* regulates autophagy in IDD, in vitro experiments were

performed using primary human NPCs. As shown in Fig. 4A, intracellular  $\text{Ca}^{2+}$  levels were significantly higher in the IL- $1\beta$ -treated group than in the control group ( $p = 0.003$ ). Following siRNA-mediated knockdown of *TRPC3*,  $\text{Ca}^{2+}$  levels were significantly reduced compared with those in the shRNA NC group ( $p = 0.050$ ). In addition, treatment of NPCs with PDTC, a selective NF- $\kappa\text{B}$  inhibitor, led to a further reduction in intracellular  $\text{Ca}^{2+}$  levels ( $p = 0.050$ ). Western blot analysis showed that knockdown of *TRPC3* attenuated the IL- $1\beta$ -induced increase in phosphorylated NF- $\kappa\text{B}$  p65 ( $p = 0.011$ ), while total NF- $\kappa\text{B}$  p65 expression remained unchanged ( $p = 0.273$ ) (Fig. 4B–D). Notably, PDTC treatment significantly suppressed p-NF- $\kappa\text{B}$  p65 phosphorylation in the presence of siRNA *TRPC3* ( $p = 0.050$ ) (Fig. 4D, Supplementary Table 3). Furthermore, siRNA-mediated knockdown of *TRPC3* increased the expression of *ATG5*, *Beclin-1*, and the *LC3-II/LC3-I* ratio compared with the IL- $1\beta$  + siRNA NC group ( $p < 0.05$ ). Moreover, NPCs treated with PDTC in combination with siRNA *TRPC3* and IL- $1\beta$  exhibited further increases in these autophagy-related proteins (all  $p = 0.050$ ) (Fig. 5A–D). In addition, PDTC significantly suppressed the IL- $1\beta$ -induced increase in *TRPC3* expression ( $p = 0.050$ ) (Fig. 5E, Supplementary Table 4). Collectively, these results indicate that *TRPC3* activates the NF- $\kappa\text{B}$  pathway through  $\text{Ca}^{2+}$  influx and promotes autophagy-related protein expression, ultimately exacerbating IDD, whereas combined inhibition of *TRPC3* and NF- $\kappa\text{B}$  exerts a synergistic effect in enhancing protective autophagy, thereby delaying IDD progression.

### The knockdown of *TRPC3*-activated autophagy promoted apoptosis in NPCs

To further examine the impact of *TRPC3*-induced autophagy on cell apoptosis, NPCs were treated with rapamycin

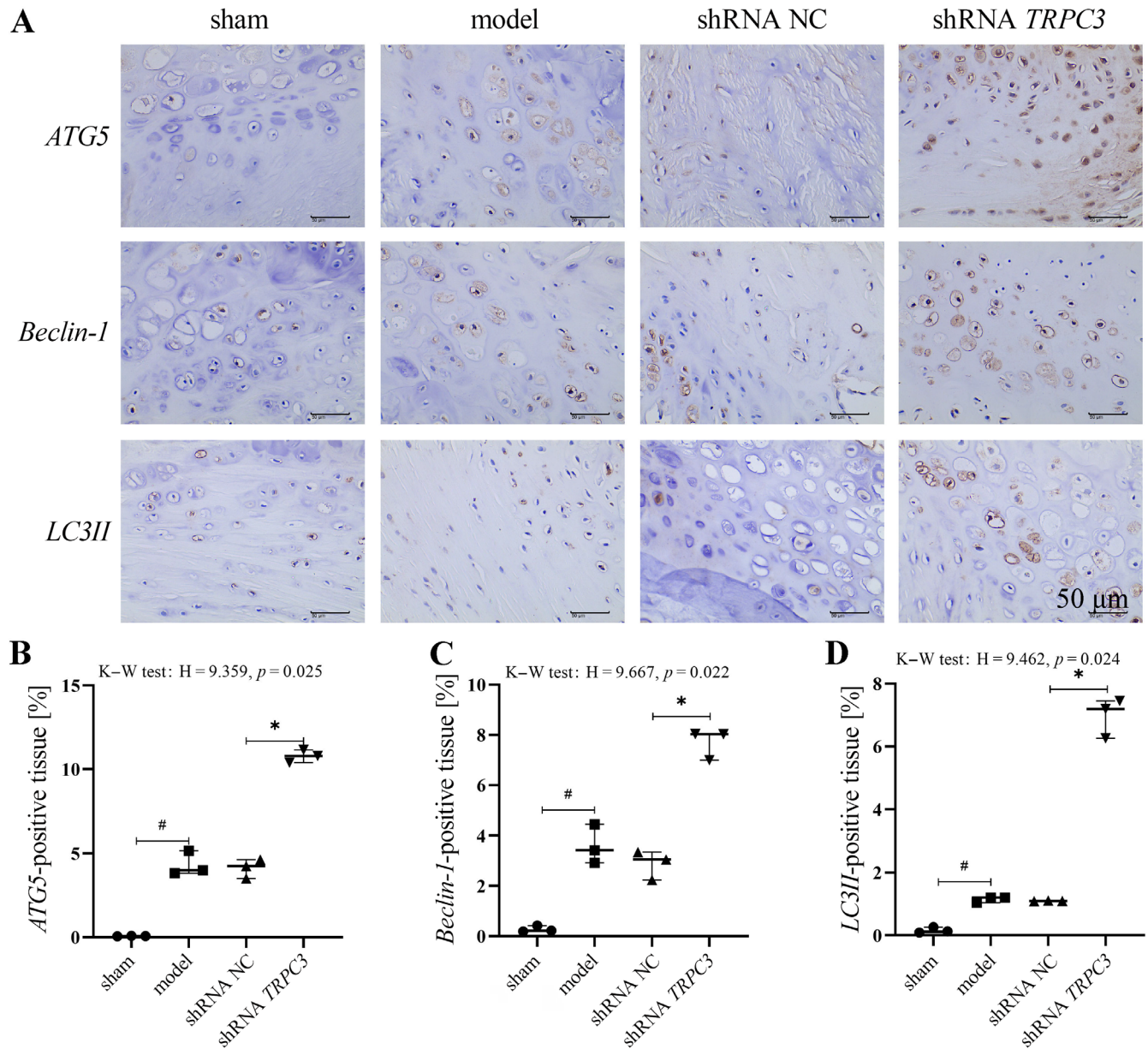


**Fig. 2.** Inhibition of *TRPC3* promotes autophagy-related protein expression in the nucleus pulposus of intervertebral discs. A. Immunohistochemical staining of *ATG5*, *Beclin-1*, and *LC3-II* in intervertebral disc tissues. Scale bar = 50  $\mu$ m. Hematoxylin staining shows cell nuclei in blue, and diaminobenzidine (DAB) staining indicates positive expression in brown; B–D. Quantitative analysis of the positive area ratios of *ATG5*, *Beclin-1*, and *LC3-II* immunohistochemical staining. Data are presented as the median (minimum–maximum) (n = 3). Data were analyzed using the Kruskal–Wallis test followed by Dunn’s post hoc test with Bonferroni correction

#p < 0.05 vs the sham group; \*p < 0.05 vs the shRNA negative control (NC) group; *TRPC3* – transient receptor potential canonical 3; DAB – diaminobenzidine; *ATG5* – autophagy-related protein 5.

(RAPA) and 3-methyladenine (3-MA). In the IL-1 $\beta$  group, TEM revealed the presence of autophagosomes and primary lysosomes, whereas the IL-1 $\beta$  + siRNA *TRPC3* group exhibited a markedly increased number of autophagosomes and primary lysosomes. Treatment with RAPA further enhanced autophagy, whereas 3-MA reduced autophagic activity (Fig. 6). Furthermore, compared with the control group, IL-1 $\beta$  treatment markedly increased NPC apoptosis (p = 0.050). Following siRNA-mediated knockdown of *TRPC3*, NPC apoptosis was significantly higher than

that in the shRNA NC group (p = 0.050). Compared with the IL-1 $\beta$  + siRNA *TRPC3* group, treatment with RAPA resulted in a further increase in NPC apoptosis (p = 0.039), whereas 3-MA led to a reduction in apoptosis (Fig. 7, Supplementary Table 5).

These results suggest that *TRPC3* alleviates IL-1 $\beta$ -induced apoptosis in NPCs by inhibiting autophagy, whereas excessive activation of autophagy exacerbates cell death, indicating a bidirectional role of the *TRPC3*-autophagy axis in the regulation of apoptosis.

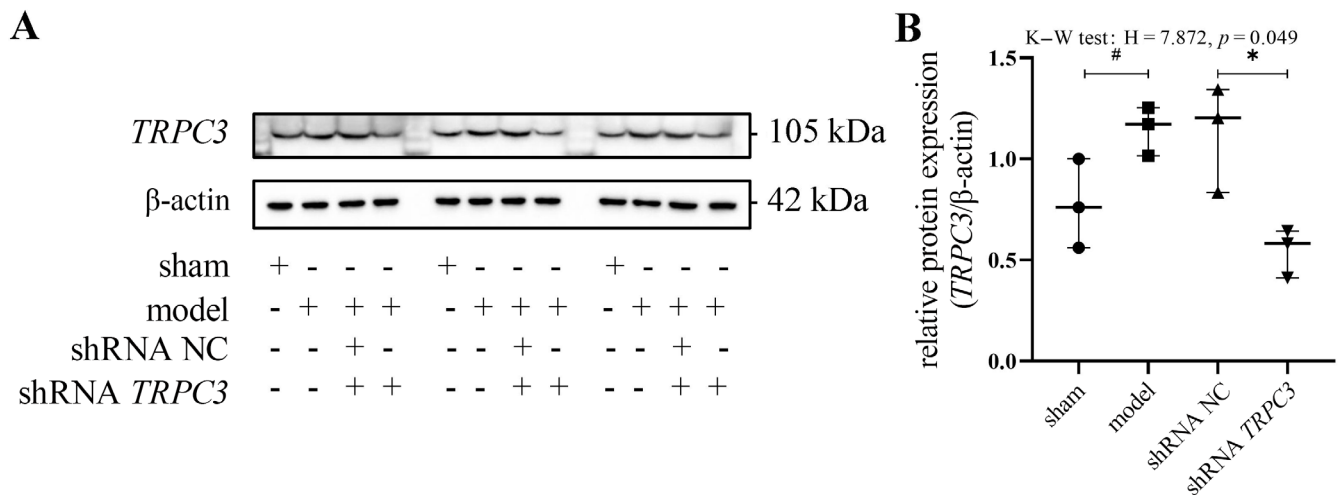


**Fig. 3.** Effect of *TRPC3* knockdown on *TRPC3* protein expression. A. *TRPC3* protein levels in intervertebral disc tissues were detected with western blot analysis; B. Quantitative analysis of *TRPC3* protein expression. Data are presented as the median (min–max) (n = 3). Data were analyzed using the Kruskal–Wallis test followed by Dunn’s post hoc test with Bonferroni correction

#p < 0.05 vs the sham group; \*p < 0.05 vs the shRNA NC group; *TRPC3* – transient receptor potential canonical 3.

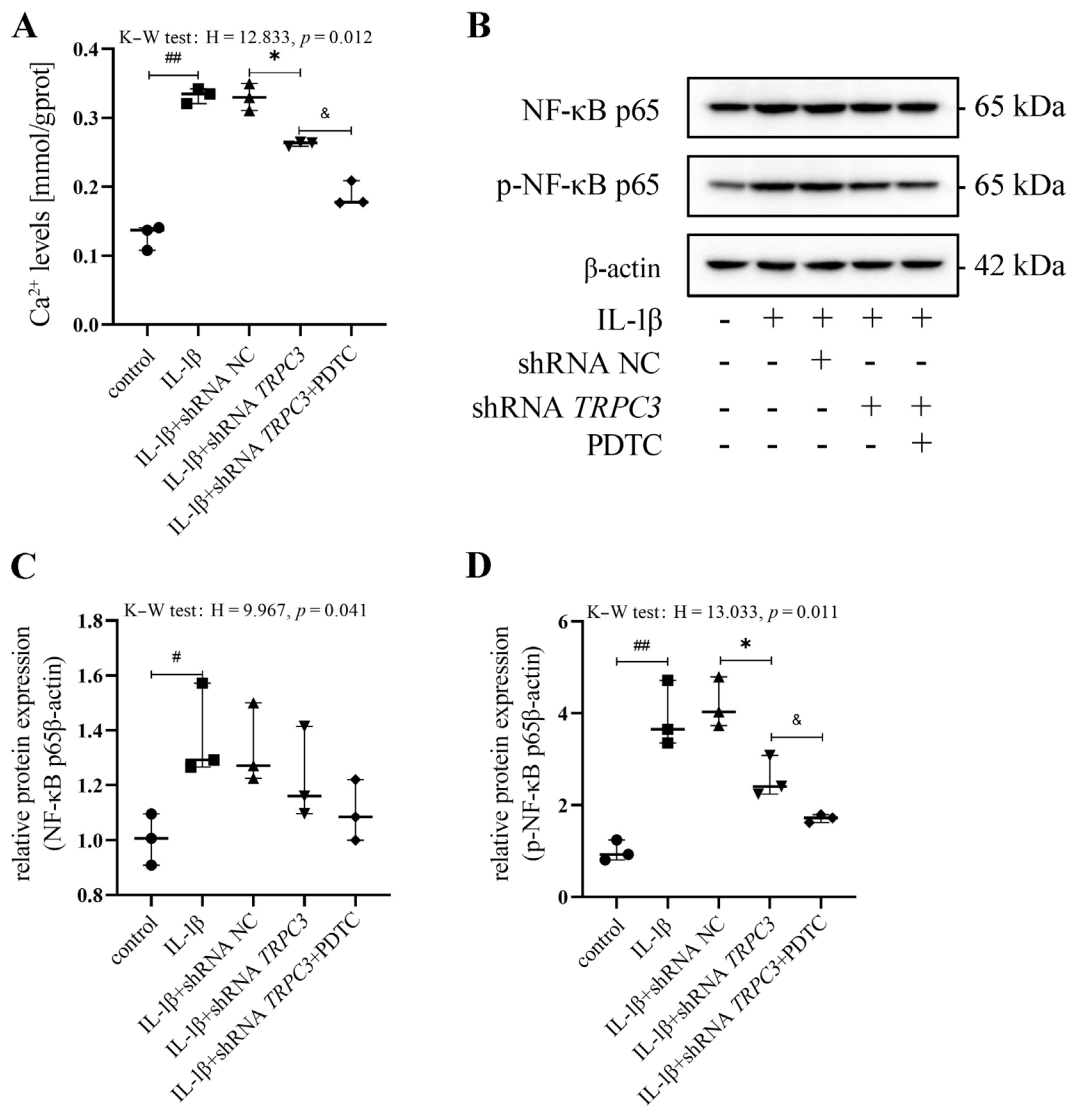


**Fig. 4.** *TRPC3* knockdown inhibits the  $Ca^{2+}$ /NF- $\kappa$ B pathway and promotes autophagy in NPCs. NPCs were pretreated with IL-1 $\beta$ , siRNA *TRPC3*, or the NF- $\kappa$ B inhibitor PDTC, respectively. A. Intracellular  $Ca^{2+}$  levels in NPCs were measured using a spectrophotometer; B. Western blot images showing NF- $\kappa$ B p65 and phosphorylated NF- $\kappa$ B p65 (p-NF- $\kappa$ B p65) protein expression in NPCs; C,D. Quantitative analysis of NF- $\kappa$ B p65 and p-NF- $\kappa$ B p65 protein expression. Data are presented as the median (minimum–maximum) (n = 3). Data were analyzed using the Kruskal–Wallis test followed by Dunn’s post hoc test with Bonferroni correction

##p < 0.01 vs the control group; \*p < 0.05 vs the IL-1 $\beta$  + siRNA NC group; §p < 0.01 vs the IL-1 $\beta$  + siRNA *TRPC3* group; *TRPC3* – transient receptor potential canonical 3; NF- $\kappa$ B – nuclear factor kappa B; IL-1 $\beta$  – interleukin-1 beta; NPCs – nucleus pulposus cells; PDTC – pyrrolidine-dithiocarbamic acid.

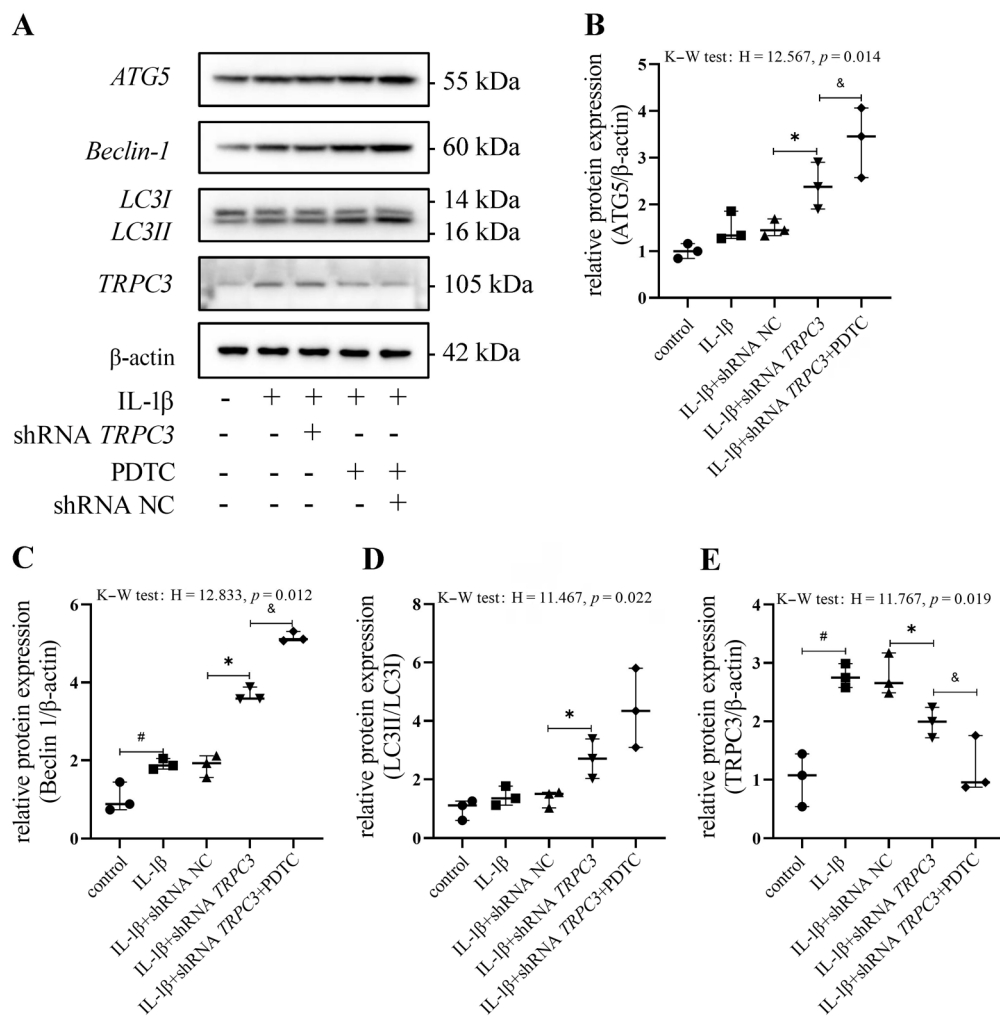


**Fig. 5.** Western blot analysis of *ATG5*, *Beclin-1*, *LC3-II/LC3-I*, and *TRPC3* expression in NPCs pretreated with *TRPC3* knockdown and the NF- $\kappa$ B inhibitor PDTC. A Representative western blot images of *ATG5*, *Beclin-1*, *LC3-II/LC3-I*, and *TRPC3* proteins; B–E Quantitative analysis of *ATG5*, *Beclin-1*, *LC3-II/LC3-I*, and *TRPC3* protein expression. Data are presented as the median (minimum–maximum) ( $n = 3$ ). Data were analyzed using the Kruskal–Wallis test followed by Dunn’s post hoc test with Bonferroni correction

# $p < 0.05$  vs the control group; \* $p < 0.05$  vs. the IL-1 $\beta$  + shRNA NC group; & $p < 0.01$  vs the IL-1 $\beta$  + siRNA *TRPC3* group; *TRPC3* – transient receptor potential canonical 3; NF- $\kappa$ B – nuclear factor kappa B; *ATG5* – autophagy-related protein 5; NPCs – nucleus pulposus cells; PDTC – pyrrolidine thiocarbamate; IL-1 $\beta$  – interleukin-1 beta; NC – negative control.

### The knockdown of *TRPC3* induced autophagy to regulate the expression of IDD-related proteins in NPCs

To investigate the regulatory effect of *TRPC3*-induced autophagy on ECM degradation in NPCs, western blot analysis was used to detect the expression levels of *MMP-13*, collagen II, and aggrecan (Fig. 8, Supplementary Table 6). Interleukin-1 beta treatment significantly reduced aggrecan ( $p = 0.007$ ) and collagen II ( $p = 0.002$ ) expression compared with the control group, while significantly increasing *MMP-13* expression ( $p = 0.002$ ). In addition, knockdown of *TRPC3* reversed these expression changes (all  $p = 0.050$ ). Compared with the IL-1 $\beta$  + siRNA *TRPC3* group, treatment with RAPA increased the expression of aggrecan and collagen II and decreased *MMP-13* expression (all  $p = 0.050$ ). In contrast, treatment with 3-MA reduced collagen II expression ( $p = 0.050$ ) and increased *MMP-13* expression ( $p = 0.050$ ), while no significant difference was observed in aggrecan expression ( $p = 0.646$ ). Taken together, these results indicate that *TRPC3* knockdown reverses IL-1 $\beta$ -induced ECM degradation by promoting autophagy in NPCs.

### Discussion

Intervertebral disc degeneration is a leading cause of LBP and neurological compression syndromes. The pathogenesis of IDD is complex and mainly involves excessive mechanical stress, increased apoptosis of NPCs abnormal ECM degradation, dysregulated autophagy, oxidative stress-induced damage, and genetic factors. *TRPC3* is a member of the TRP family of cation channels, which are involved in various physiological processes, including calcium homeostasis and cell signaling. This study elucidates a novel role of *TRPC3* in IDD pathogenesis, demonstrating that *TRPC3* exacerbates disc degeneration by orchestrating  $Ca^{2+}$ /NF- $\kappa$ B-mediated suppression of autophagy, thereby providing a new research direction for targeted therapy of IDD.

The intervertebral disc is principally composed of 3 distinct components: the central gelatinous NP, the outer fibrous annulus fibrosus (AF), and the cartilaginous endplate (CEP).<sup>35</sup> The NP is predominantly composed of water, proteoglycans, and collagen, along with substantial amounts of elastic proteins, fibronectin, and laminin. In contrast, the AF is primarily composed of collagen fibers

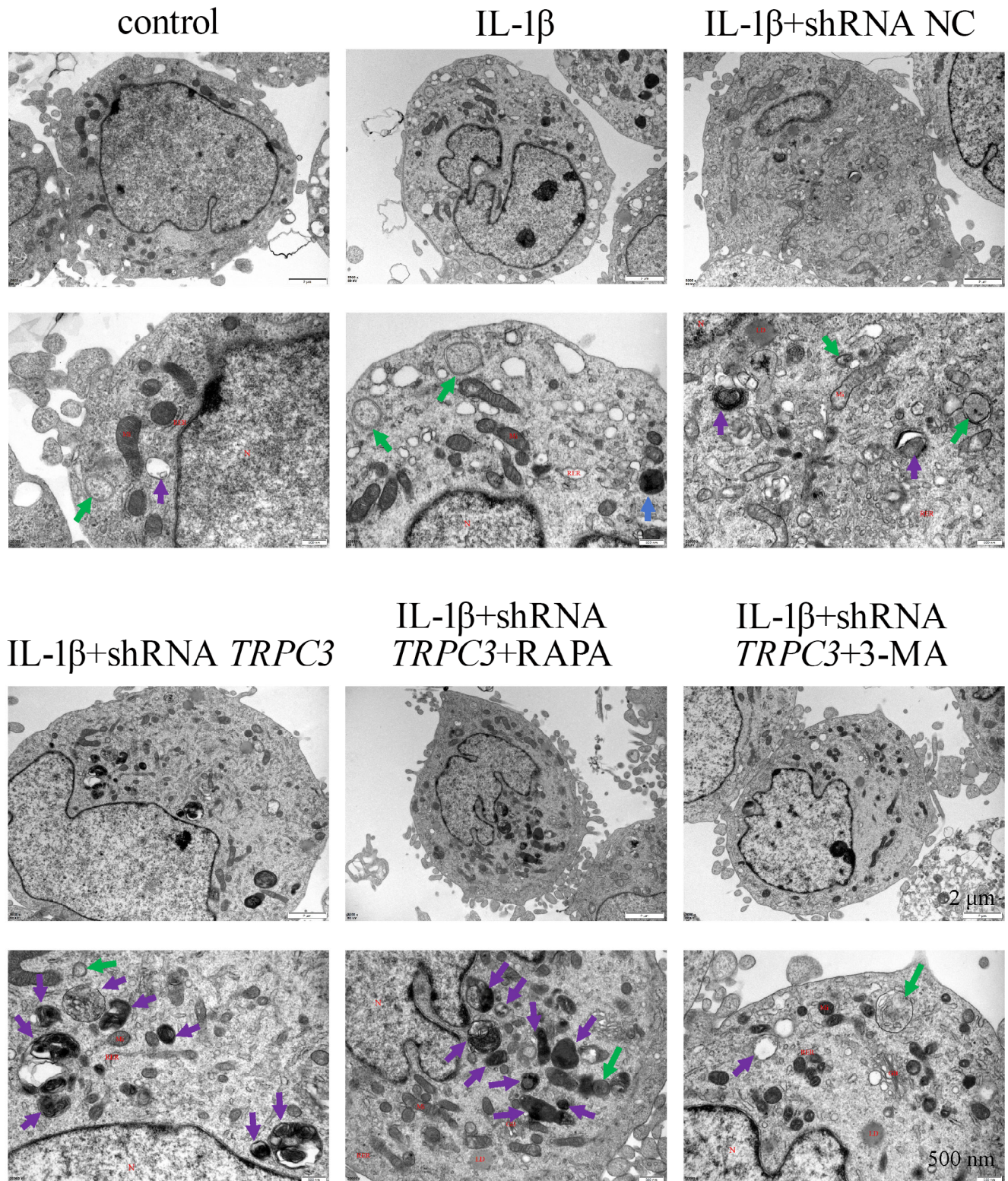


**Fig. 6.** Effect of *TRPC3* knockdown on autophagy in NPCs treated with IL-1 $\beta$ , siRNA *TRPC3*, the autophagy activator rapamycin (RAPA), and the autophagy inhibitor 3-methyladenine (3-MA). Transmission electron microscopy (TEM) images show that *TRPC3* knockdown enhances the formation of autophagosomes and primary lysosomes. Green arrows indicate autophagosomes, and purple arrows indicate autolysosomes. Scale bars = 2  $\mu$ m and 500 nm

*TRPC3* – transient receptor potential canonical 3; NPCs – nucleus pulposus cells; NC – negative control; 3-MA – 3-methyl adenine.

rich in type I collagen, whereas the CEP consists of hyaline cartilage.<sup>36,37</sup> In animal models, intervertebral disc tissue in IDD rats exhibits significant structural damage,

including a reduction in NPCs, disorganized arrangement of the AF, and abnormal deposition of cartilaginous matrix. Inhibition of *TRPC3* ameliorates these pathological

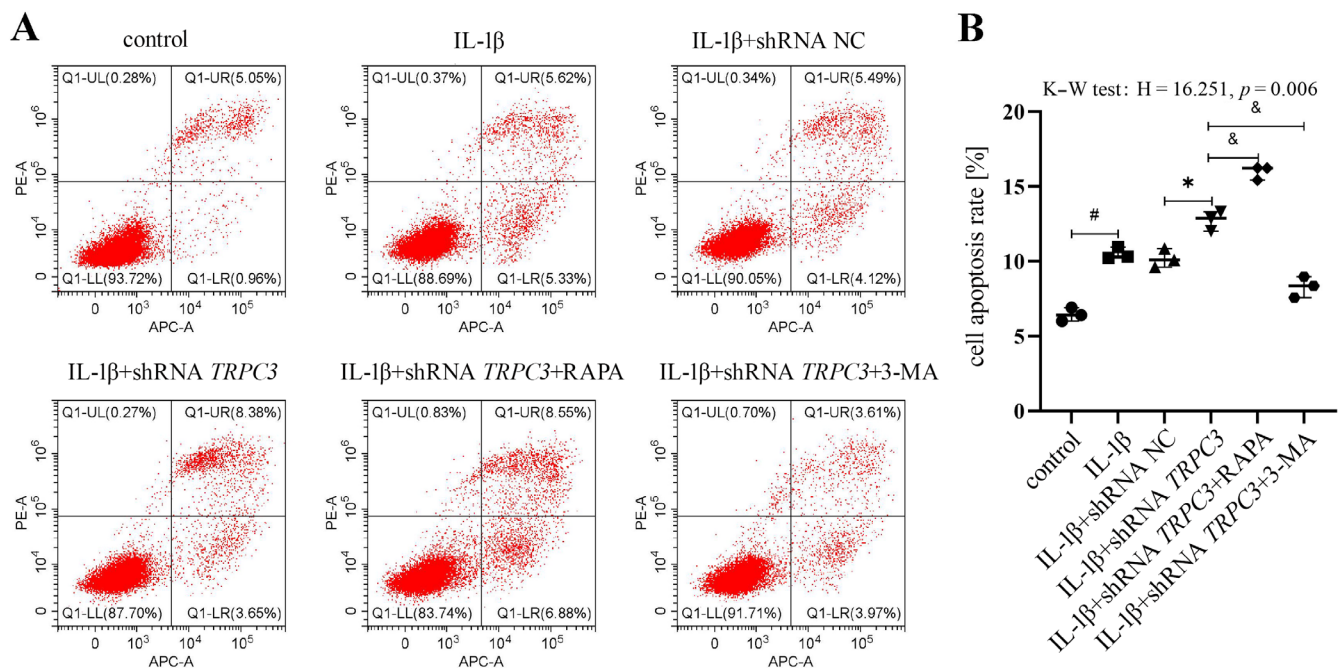


**Fig. 7.** Effect of *TRPC3* knockdown on apoptosis in NPCs. Cells were transiently transfected with siRNA negative control (NC) or siRNA *TRPC3* and then treated with IL-1β, the autophagy activator rapamycin (RAPA), or the autophagy inhibitor 3-methyladenine (3-MA), respectively. Apoptosis was analyzed with flow cytometry. Representative flow cytometry plots and quantitative results are shown. The Q1-UR region represents late apoptotic cells, Q1-UL represents necrotic cells, Q1-LL represents viable cells, and Q1-LR represents early apoptotic cells. Data are presented as the median (minimum–maximum) (n = 3). Data were analyzed using the Kruskal–Wallis test followed by Dunn’s post hoc test with Bonferroni correction

#p < 0.05 vs. the control group; \*p < 0.05 vs. the IL-1β + shRNA NC group; &p < 0.05 vs. the IL-1β + siRNA *TRPC3* group; *TRPC3* – transient receptor potential canonical 3; NPCs – nucleus pulposus cells; IL-1β – interleukin-1 beta.

changes in rat intervertebral disc tissue. These findings suggest that *TRPC3* primarily influences the progression of IDD by regulating cellular functions, such as autophagy and apoptosis, rather than by directly affecting bone structure. Consistent with this, previous studies have shown that members of the TRP channel family, such as TRPV4, regulate ECM homeostasis through ion channel activity in chondrocyte metabolism rather than directly modulating bone remodeling, thereby supporting the conclusions of the present study.<sup>38</sup>

Autophagy is a crucial cellular process that maintains homeostasis by degrading damaged components through lysosomes and plays a dual role in IDD: moderate autophagy eliminates damaged organelles and protects NPCs, whereas excessive autophagy may induce apoptosis.<sup>19</sup> ATG5 is a key regulator of autophagy, facilitating autophagosome formation and promoting autophagic flux.<sup>39,40</sup> The initiation of autophagy largely depends on *Beclin-1*, and *LC3-II* is commonly used as a marker of autophagy.<sup>41–43</sup> Our study reveals that under IL-1β stimulation, overexpression of *TRPC3* leads to a compensatory upregulation of the autophagy markers *ATG5*, *Beclin-1*, and *LC3-II*, accompanied by ECM degradation, as evidenced by downregulation of collagen II and aggrecan and upregulation of *MMP-13*. These findings suggest that *TRPC3* may cause abnormal accumulation of autophagosomes by blocking autophagic flux, possibly due to impaired lysosomal function. Further experiments confirmed that

*TRPC3* knockdown or treatment with the autophagy inducer RAPA significantly restored autophagic activity and reversed ECM degradation, whereas the autophagy inhibitor 3-MA exacerbated matrix damage. Together, these results indicate that *TRPC3* promotes ECM metabolic imbalance by inhibiting protective autophagy, and that restoration of autophagic flux may be critical for delaying IDD.

Mechanistically, *TRPC3* acts as a nonselective cation channel, and its activation leads to intracellular Ca<sup>2+</sup> overload.<sup>44</sup> Our data demonstrate that IL-1β stimulation significantly elevates intracellular Ca<sup>2+</sup> levels in human NPCs, an effect that is effectively mitigated by *TRPC3* knockdown. This Ca<sup>2+</sup> overload correlates with enhanced phosphorylation of NF-κB p65, suggesting that *TRPC3*-mediated Ca<sup>2+</sup> influx is a critical activator of NF-κB signaling. In addition, Ca<sup>2+</sup> may activate the IκB kinase (IKK) complex via calcium/calmodulin-dependent protein kinase II (CaMKII), thereby promoting IκBα degradation and subsequent nuclear translocation of NF-κB.<sup>45</sup> Notably, the NF-κB inhibitor PDTC not only suppressed p-NF-κB p65 phosphorylation but also attenuated IL-1β-induced *TRPC3* upregulation, revealing a self-reinforcing “*TRPC3*–Ca<sup>2+</sup>–NF-κB–*TRPC3*” positive feedback loop. This vicious cycle amplifies apoptotic responses and ECM degradation, thereby promoting IDD progression. Knockdown of *TRPC3* or treatment with the NF-κB inhibitor PDTC reversed this phenomenon and synergistically enhanced the expression of *ATG5*, *Beclin-1*,

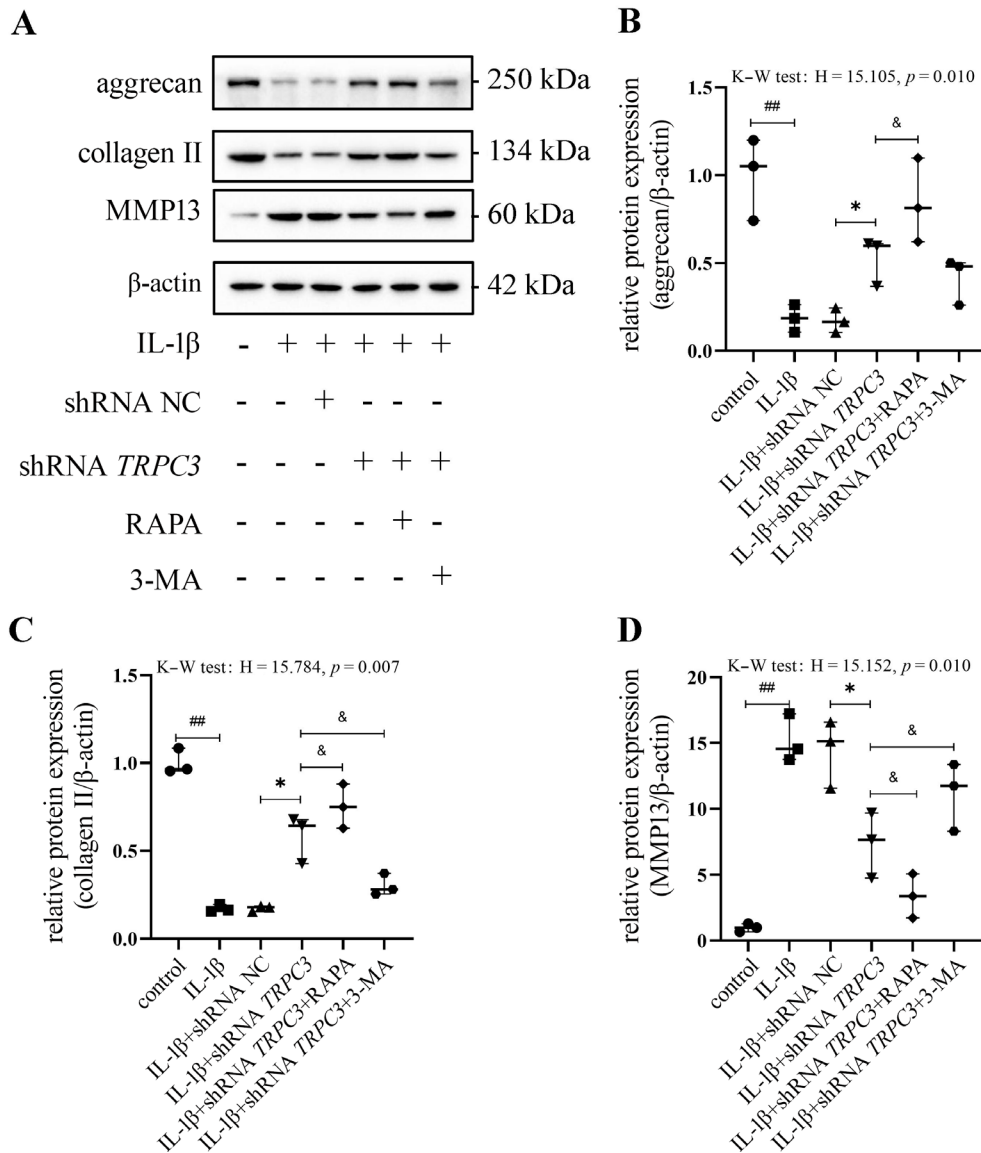


**Fig. 8.** *TRPC3* knockdown induces autophagy to regulate the expression of IDD-related proteins in NPCs. **A** Representative western blot images of *MMP-13*, collagen II, and aggrecan proteins; **B–D** Quantitative analysis of *MMP-13*, collagen II, and aggrecan protein expression. Data are presented as the median (minimum–maximum) ( $n = 3$ ). Data were analyzed using the Kruskal–Wallis test followed by Dunn’s post hoc test with Bonferroni correction

##  $p < 0.01$  vs the control group; \*  $p < 0.05$  vs the IL-1β + shRNA negative control (NC) group; &  $p < 0.05$  vs the IL-1β + siRNA *TRPC3* group; *TRPC3* – transient receptor potential canonical 3; NPCs – nucleus pulposus cells; IDD – intervertebral disc degeneration; *MMP-13* – matrix metalloproteinase-13; IL-1β – interleukin-1 beta.

and *LC3-II*. These findings suggest that *TRPC3* negatively regulates autophagy through the  $Ca^{2+}/NF-\kappa B$  axis, and that the underlying mechanism may involve  $NF-\kappa B$ -mediated transcriptional repression of autophagy-related genes, such as the *ATG5* promoter.<sup>46</sup>

One of the characteristic features of IDD is apoptosis of NPCs.<sup>47</sup> The interplay between autophagy and apoptosis has attracted considerable attention in IDD research. In this study, we observed that IL-1β-induced apoptosis in NPCs was further exacerbated by *TRPC3* knockdown. In addition, the autophagy activator RAPA enhanced apoptosis, whereas the autophagy inhibitor 3-MA attenuated apoptotic responses. These findings suggest bidirectional regulation of autophagy at different stages: moderate autophagy inhibits apoptosis by clearing damaged mitochondria, whereas excessive autophagy – such as “autophagic stress” caused by impaired autophagic flux – may promote apoptosis by activating caspase pathways or depleting pro-survival signals.<sup>48</sup> *TRPC3* knockdown may trigger this

latter effect by inducing excessive autophagy, including accumulation of autophagosomes.

Extracellular matrix degradation is a central feature of IDD,<sup>49</sup> primarily driven by an imbalance among MMPs, aggrecan, and collagen II. During the early stages of IDD, there is a notable increase in the production of type II collagen in the NP, suggesting an attempt by the tissue to initiate repair mechanisms. As degeneration progresses, type II collagen content markedly decreases, while type I collagen forms more pronounced fibrous structures in the AF and NP.<sup>50</sup> In addition, a key hallmark of degeneration is alteration of proteoglycans, particularly degradation of aggrecan, a major polymeric proteoglycan of the intervertebral disc.<sup>51</sup> Aggrecan, with its glycosaminoglycan side chains containing numerous negatively charged groups, confers unique permeability to the NP, allowing it to maintain a swollen state under compressive loads.<sup>52</sup> Moreover, recent studies have demonstrated that ECM degradation is an early and critical event in IDD,

involving metalloproteinases such as *MMP-1*, *MMP-3*, and *MMP-13*, which play key roles and are considered risk genes associated with disc degeneration.<sup>53,54</sup> Our study demonstrates that *TRPC3* knockdown reverses IL-1 $\beta$ -induced upregulation of *MMP-13* and downregulation of collagen II and aggrecan by activating autophagy. Mechanistically, autophagy may maintain ECM homeostasis through several pathways: 1) degrading damaged MMP precursors<sup>55</sup>; 2) inhibiting NF- $\kappa$ B-mediated *MMP-13* transcription via the mTORC1 pathway<sup>56</sup>; and 3) enhancing the anabolic function of NPCs to promote secretion of ECM components.<sup>57</sup> Notably, the autophagy inhibitor 3-MA partially reverses the protective effects of *TRPC3* knockdown on the ECM, further supporting the central role of autophagy. In addition, NF- $\kappa$ B, as a key transcription factor regulating *MMP-13* expression, may directly reduce ECM degradation when inhibited, while *TRPC3* knockdown exerts a synergistic protective effect through a dual mechanism involving autophagy activation and NF- $\kappa$ B inhibition.

## Limitations of the study

This study has several limitations. First, we only conducted an initial exploration of the role of *TRPC3* in IDD. In addition, the rat IDD model cannot fully recapitulate the chronic degenerative process observed in humans; therefore, the effects and underlying mechanisms of *TRPC3* on ECM metabolism in IDD in vivo require further investigation. Although this study elucidates the mechanism by which *TRPC3* regulates autophagy through the Ca<sup>2+</sup>/NF- $\kappa$ B pathway, the pathophysiology of IDD is complex and multifactorial, potentially involving multiple signaling pathways and molecular mechanisms beyond those examined here. Future research should explore additional signaling pathways and molecular mechanisms involved in IDD and their relationships with *TRPC3*. In addition, the potential involvement of other Ca<sup>2+</sup> channels, such as *TRPV4*, cannot be excluded and warrants further validation of the functional specificity of *TRPC3* using gene-editing approaches, such as CRISPR–Cas9.

## Conclusions

The results of this study indicate that *TRPC3* promotes autophagy by regulating the Ca<sup>2+</sup>/NF- $\kappa$ B pathway, induces apoptosis of NPCs and ECM degradation, and thereby contributes to the development of IDD. These findings highlight the importance of *TRPC3* as a key therapeutic target in IDD and provide potential strategies for the treatment of this condition.

Future studies may focus on the development of small-molecule drugs targeting *TRPC3*, particularly highly selective *TRPC3* inhibitors, as well as the application

of nanodelivery technologies to enhance the clinical translation potential of *TRPC3*-targeted therapies for IDD. In addition, exploring combination strategies involving *TRPC3* inhibitors together with NF- $\kappa$ B antagonists or autophagy modulators may synergistically enhance the suppression of IDD progression.

## Supplementary files

The supplementary materials are available at <https://doi.org/10.5281/zenodo.16352711>. The package contains the following files:

Supplementary Table 1. Kruskal–Wallis test results for Fig. 2.

Supplementary Table 2. Kruskal–Wallis test results for Fig. 3.

Supplementary Table 3. Kruskal–Wallis test results for Fig. 4.

Supplementary Table 4. Kruskal–Wallis test results for Fig. 5.

Supplementary Table 5. Kruskal–Wallis test results for Fig. 7.

Supplementary Table 6. Kruskal–Wallis test results for Fig. 8.

## Data Availability Statement

The raw data of the current study are openly available in Zenodo repository at <https://doi.org/10.5281/zenodo.16352556>.

## Consent for publication

Not applicable.

## Use of AI and AI-assisted technologies

Not applicable.

## ORCID iDs

Yingchao Gao: <https://orcid.org/0009-0001-4869-9952>

Ning Zhang: <https://orcid.org/0009-0009-5142-9142>

Jun-Fei Zhang: <https://orcid.org/0000-0003-0575-4955>

Zhengqi Fei: <https://orcid.org/0009-0000-1266-3555>

## References

- Xin J, Wang Y, Zheng Z, Wang S, Na S, Zhang S. Treatment of intervertebral disc degeneration. *Orthop Surg.* 2022;14(7):1271–1280. doi:10.1111/os.13254
- Kamali A, Ziadlou R, Lang G, et al. Small molecule-based treatment approaches for intervertebral disc degeneration: Current options and future directions. *Theranostics.* 2021;11(1):27–47. doi:10.7150/thno.48987
- Diwan AD, Melrose J. Intervertebral disc degeneration and how it leads to low back pain. *JOR Spine.* 2023;6(1):e1231. doi:10.1002/jsp2.1231
- Xia Q, Zhao Y, Dong H, et al. Progress in the study of molecular mechanisms of intervertebral disc degeneration. *Biomed Pharmacother.* 2024;174:116593. doi:10.1016/j.biopha.2024.116593

5. Shen Y, Jiang Y, Jiang R, et al. Intervertebral disc degeneration mediates the causal effect of genetically predicted diffuse idiopathic skeletal hyperostosis on spinal stenosis: Evidence from a Mendelian randomization study. *JOR Spine*. 2025;8(1):e70041. doi:10.1002/jsp2.70041
6. Wang Y, Cheng H, Wang T, Zhang K, Zhang Y, Kang X. Oxidative stress in intervertebral disc degeneration: Molecular mechanisms, pathogenesis and treatment. *Cell Prolif*. 2023;56(9):e13448. doi:10.1111/cpr.13448
7. Fatoye F, Gebrye T, Ryan CG, Useh U, Mbada C. Global and regional estimates of clinical and economic burden of low back pain in high-income countries: A systematic review and meta-analysis. *Front Public Health*. 2023;11:1098100. doi:10.3389/fpubh.2023.1098100
8. Liu P, Ren X, Zhang B, Guo S, Fu Q. Investigating the characteristics of mild intervertebral disc degeneration at various age stages using single-cell genomics. *Front Cell Dev Biol*. 2024;12:1409287. doi:10.3389/fcell.2024.1409287
9. Yan SM, Han BQ, Song C, Yan LM. Molecular mechanisms and treatment strategies for discogenic lumbar pain. *Immunol Res*. 2025;73(1):111. doi:10.1007/s12026-025-09667-w
10. Song C, Hu P, Peng R, Li F, Fang Z, Xu Y. Bioenergetic dysfunction in the pathogenesis of intervertebral disc degeneration. *Pharmacol Res*. 2024;202:107119. doi:10.1016/j.phrs.2024.107119
11. Yurube T, Ito M, Kakiuchi Y, Kuroda R, Kakutani K. Autophagy and mTOR signaling during intervertebral disc aging and degeneration. *JOR Spine*. 2020;3(1):e1082. doi:10.1002/jsp2.1082
12. Wang Z, Li X, Yu P, et al. Role of autophagy and pyroptosis in intervertebral disc degeneration. *J Inflamm Res*. 2024;17:91–100. doi:10.2147/JIR.S434896
13. Liang H, Luo R, Li G, Zhang W, Song Y, Yang C. The proteolysis of ECM in intervertebral disc degeneration. *Int J Mol Sci*. 2022;23(3):1715. doi:10.3390/ijms23031715
14. Bianchi S, Bernardi S, Mattei A, et al. Morphological and biological evaluations of human periodontal ligament fibroblasts in contact with different bovine bone grafts treated with low-temperature deproteinisation protocol. *Int J Mol Sci*. 2022;23(9):5273. doi:10.3390/ijms23095273
15. Lu X, Lin Z, Li L, et al. Exosome-loaded methacrylated silk fibroin hydrogel delays intervertebral disc degeneration by DKK2-mediated mitochondrial unfolded protein response. *Chem Eng J*. 2025;511:162191. doi:10.1016/j.cej.2025.162191
16. Liu Y, Levine B. Autosis and autophagic cell death: The dark side of autophagy. *Cell Death Differ*. 2015;22(3):367–376. doi:10.1038/cdd.2014.143
17. Wang W, Sun Y, Tang P, et al. CircTBCK protects against osteoarthritis by regulating extracellular matrix and autophagy. *Human Cell*. 2025;38(2):60. doi:10.1007/s13577-025-01186-y
18. Zhang TW, Li ZF, Dong J, Jiang LB. The circadian rhythm in intervertebral disc degeneration: An autophagy connection. *Exp Mol Med*. 2020;52(1):31–40. doi:10.1038/s12276-019-0372-6
19. Kritschil R, Scott M, Sowa G, Vo N. Role of autophagy in intervertebral disc degeneration. *J Cell Physiol*. 2022;237(2):1266–1284. doi:10.1002/jcp.30631
20. Cheng ZR, Gan WK, Xiang Q, et al. Impaired degradation of PLCG1 by chaperone-mediated autophagy promotes cellular senescence and intervertebral disc degeneration. *Autophagy*. 2025;21(2):352–373. doi:10.1080/15548627.2024.2395797
21. Gruber HE, Hoelscher GL, Ingram JA, Bethea S, Hanley EN. Autophagy in the degenerating human intervertebral disc: In vivo molecular and morphological evidence, and induction of autophagy in cultured annulus cells exposed to proinflammatory cytokines. Implications for disc degeneration. *Spine (Phila Pa 1976)*. 2015;40(11):773–782. doi:10.1097/BRS.0000000000000865
22. Xie C, Shi Y, Chen Z, et al. Apigenin alleviates intervertebral disc degeneration via restoring autophagy flux in nucleus pulposus cells. *Front Cell Dev Biol*. 2022;9:787278. doi:10.3389/fcell.2021.787278
23. Zhang SJ, Yang W, Wang C, et al. Autophagy: A double-edged sword in intervertebral disk degeneration. *Clin Chim Acta*. 2016;457:27–35. doi:10.1016/j.cca.2016.03.016
24. Casas J, Meana C, López-López JR, Balsinde J, Balboa MA. Lipin-1-derived diacylglycerol activates intracellular TRPC3 which is critical for inflammatory signaling. *Cell Mol Life Sci*. 2021;78(24):8243–8260. doi:10.1007/s00018-021-03999-0
25. Song T, Hao Q, Zheng YM, Liu QH, Wang YX. Inositol 1,4,5-trisphosphate activates TRPC3 channels to cause extracellular Ca<sup>2+</sup> influx in airway smooth muscle cells. *Am J Physiol Lung Cell Mol Physiol*. 2015;309(12):L1455–L1466. doi:10.1152/ajplung.00148.2015
26. Klein S, Mentrup B, Timmen M, et al. Modulation of transient receptor potential channels 3 and 6 regulates osteoclast function with impact on trabecular bone loss. *Calcif Tissue Int*. 2020;106(6):655–664. doi:10.1007/s00223-020-00673-8
27. Kim JE, Kim SY, Lim SY, Kieff E, Song YJ. Role of Ca<sup>2+</sup>/calmodulin-dependent kinase II–IRAK1 interaction in LMP1-induced NF-κB activation. *Mol Cell Biol*. 2014;34(3):325–334. doi:10.1128/MCB.00912-13
28. Cheng P, Wei H, Chen H, Wang Z, Mao P, Zhang H. DNMT3-mediated methylation of PPARγ promote intervertebral disc degeneration by regulating the NF-κB pathway. *J Cell Mol Med*. 2024;28(2):e18048. doi:10.1111/jcmm.18048
29. Chen F, Liu H, Wang X, et al. Melatonin activates autophagy via the NF-κB signaling pathway to prevent extracellular matrix degeneration in intervertebral disc. *Osteoarthritis Cartilage*. 2020;28(8):1121–1132. doi:10.1016/j.joca.2020.05.011
30. Sun Z, Tang X, Wang H, et al. LncRNA H19 aggravates intervertebral disc degeneration by promoting the autophagy and apoptosis of nucleus pulposus cells through the miR-139/CXCR4/NF-κB axis. *Stem Cells Dev*. 2021;30(14):736–748. doi:10.1089/scd.2021.0009
31. Huang Y, Wang L, Luo B, et al. Associations of lumbar disc degeneration with paraspinal muscles myosteatosis in discogenic low back pain. *Front Endocrinol (Lausanne)*. 2022;13:891088. doi:10.3389/fendo.2022.891088
32. Zou Z, Hu X, Luo T, et al. Naturally-occurring spinosyn A and its derivatives function as argininosuccinate synthase activator and tumor inhibitor. *Nat Commun*. 2021;12(1):2263. doi:10.1038/s41467-021-22235-8
33. Zou R, Shi W, Chang X, et al. The DNA-dependent protein kinase catalytic subunit exacerbates endotoxemia-induced myocardial microvascular injury by disrupting the MOTS-c/JNK pathway and inducing profilin-mediated lamellipodia degradation. *Theranostics*. 2024;14(4):1561–1582. doi:10.7150/thno.92650
34. Lee Y, DiMauro-Milk E, Leslie J, Ding L. Hematopoietic stem cells temporally transition to thrombopoietin dependence in the fetal liver. *Sci Adv*. 2022;8(11):eabm7688. doi:10.1126/sciadv.abm7688
35. Sun Z, Liu B, Luo ZJ. The immune privilege of the intervertebral disc: Implications for intervertebral disc degeneration treatment. *Int J Med Sci*. 2020;17(5):685–692. doi:10.7150/ijms.42238
36. Marfia G, Campanella R, Navone SE, et al. Potential use of human adipose mesenchymal stromal cells for intervertebral disc regeneration: A preliminary study on biglycan-deficient murine model of chronic disc degeneration. *Arthritis Res Ther*. 2014;16(5):457. doi:10.1186/s13075-014-0457-5
37. Lakstins K, Arnold L, Gunsch G, et al. Characterization of the human intervertebral disc cartilage endplate at the molecular, cell, and tissue levels. *J Orthop Res*. 2021;39(9):1898–1907. doi:10.1002/jor.24854
38. O'Conor CJ, Leddy HA, Benefield HC, Liedtke WB, Guilak F. TRPV4-mediated mechanotransduction regulates the metabolic response of chondrocytes to dynamic loading. *Proc Natl Acad Sci U S A*. 2014;111(4):1316–1321. doi:10.1073/pnas.1319569111
39. Wang F, Trotsdal ES, Paddar MA, et al. The role of ATG5 beyond Atg8ylation and autophagy. *Autophagy*. 2024;20(2):448–450. doi:10.1080/15548627.2023.2273703
40. Changotra H, Kaur S, Yadav SS, Gupta GL, Parkash J, Duseja A. ATG5: A central autophagy regulator implicated in various human diseases. *Cell Biochem Funct*. 2022;40(7):650–667. doi:10.1002/cbf.3740
41. Li G, Rao H, Xu W. Puerarin plays a protective role in chondrocytes by activating Beclin1-dependent autophagy. *Biosci Biotechnol Biochem*. 2021;85(3):621–625. doi:10.1093/bbb/zbba078
42. Zhang Y, Cui Y, Wang L, Han J. Autophagy promotes osteoclast podosome disassembly and cell motility through the interaction of kindlin3 with LC3. *Cell Signal*. 2020;67:109505. doi:10.1016/j.cellsig.2019.109505
43. Quan M, Hong M, Ko M, Kim Y. Relationships between disc degeneration and autophagy expression in human nucleus pulposus. *Orthop Surg*. 2020;12(1):312–320. doi:10.1111/os.12573
44. Fliniaux I, Germain E, Farfariello V, Prevarskaya N. TRPs and Ca<sup>2+</sup> in cell death and survival. *Cell Calcium*. 2018;69:4–18. doi:10.1016/j.ceca.2017.07.002

45. Li T, Meng Y, Ding P, et al. Pathological implication of CaMKII in NF- $\kappa$ B pathway and SASP during cardiomyocytes senescence. *Mech Ageing Dev.* 2023;209:111758. doi:10.1016/j.mad.2022.111758
46. Peng X, Wang Y, Li H, et al. ATG5-mediated autophagy suppresses NF- $\kappa$ B signaling to limit epithelial inflammatory response to kidney injury. *Cell Death Dis.* 2019;10(4):253. doi:10.1038/s41419-019-1483-7
47. Wang D, He X, Wang D, et al. Quercetin suppresses apoptosis and attenuates intervertebral disc degeneration via the SIRT1-autophagy pathway. *Front Cell Dev Biol.* 2020;8:613006. doi:10.3389/fcell.2020.613006
48. Lee DY, Bahar ME, Kim CW, et al. Autophagy in osteoarthritis: A double-edged sword in cartilage aging and mechanical stress response. A systematic review. *J Clin Med.* 2024;13(10):3005. doi:10.3390/jcm13103005
49. Kaneda G, Zila L, Wechsler JT, et al. What a pain in the back: Etiology, diagnosis and future treatment directions for discogenic low back pain. *Bone Res.* 2025;13(1):89. doi:10.1038/s41413-025-00472-7
50. Hua WB, Wu XH, Zhang YK, et al. Dysregulated miR-127-5p contributes to type II collagen degradation by targeting matrix metalloproteinase-13 in human intervertebral disc degeneration. *Biochimie.* 2017;139:74–80. doi:10.1016/j.biochi.2017.05.018
51. Gruber HE, Hoelscher GL, Ingram JA, Bethea S, Zinchenko N, Hanley EN. Variations in aggrecan localization and gene expression patterns characterize increasing stages of human intervertebral disk degeneration. *Exp Mol Pathol.* 2011;91(2):534–539. doi:10.1016/j.yexmp.2011.06.001
52. Sivan SS, Wachtel E, Roughley P. Structure, function, aging and turnover of aggrecan in the intervertebral disc. *Biochim Biophys Acta Gen Subj.* 2014;1840(10):3181–3189. doi:10.1016/j.bbagen.2014.07.013
53. Basaran R, Senol M, Ozkanli S, Efendioglu M, Kaner T. Correlation of matrix metalloproteinase (MMP)-1, -2, -3, and -9 expressions with demographic and radiological features in primary lumbar intervertebral disc disease. *J Clin Neurosci.* 2017;41:46–49. doi:10.1016/j.jocn.2017.03.001
54. Zou X, Zhang X, Han S, et al. Pathogenesis and therapeutic implications of matrix metalloproteinases in intervertebral disc degeneration: A comprehensive review. *Biochimie.* 2023;214:27–48. doi:10.1016/j.biochi.2023.05.015
55. Li WD, Li NP, Song DD, Rong JJ, Qian AM, Li XQ. Metformin inhibits endothelial progenitor cell migration by decreasing matrix metalloproteinases, MMP-2 and MMP-9, via the AMPK/mTOR/autophagy pathway. *Int J Mol Med.* 2017;39(5):1262–1268. doi:10.3892/ijmm.2017.2929
56. Huang P, Dong RY, Wang P, Xu M, Sun X, Dong XP. MCOLN/TRPML channels in the regulation of MTORC1 and autophagy. *Autophagy.* 2024;20(5):1203–1204. doi:10.1080/15548627.2023.2300922
57. Wang K, Yao D, Li Y, et al. TAK-715 alleviated IL-1 $\beta$ -induced apoptosis and ECM degradation in nucleus pulposus cells and attenuated intervertebral disc degeneration ex vivo and in vivo. *Arthritis Res Ther.* 2023;25(1):45. doi:10.1186/s13075-023-03028-4